

Computation of Global Voltage Stability Margin in a Practical Power Network Incorporating FACTS in the OPF Frame Work

P. Nagendra, S. Halder nee Dey, S. Paul, T. Datta

Abstract—This paper presents a methodology to assess the voltage stability status combined with optimal power flow technique using an instantaneous two-bus equivalent model of power system incorporating static var compensator (SVC) and thyristor controlled series compensator (TCSC) controllers. There by, a generalized global voltage stability indicator being developed has been applied to a robust practical Indian Eastern Grid 203-bus system. Simulation results have proved that the proposed methodology is promising to assess voltage stability of any power system at any operating point in global scenario. Voltage stability augmentation with the application of SVC at the weakest bus and TCSC at critical line connected to the weakest bus is compared with the system having no compensation. In the proposed network equivalent model the generators have been modeled more accurately considering economic criteria.

Keywords—Equivalent two-bus model, global voltage security indicator, optimal power flow, SVC, TCSC.

I. INTRODUCTION

PRESENT day power systems are operating very much closer to their limits of stability to meet the continued growth of load demand with limited transmission and/or generation enhancement due to economic and environmental problems. This leads to stability and security problems of the system operation. Voltage stability is one of these concerns and is refer to the ability of a power system to maintain acceptable voltage at all buses in the system under normal conditions or after being subjected to a disturbance [1]. A system is in a state of voltage instability when a disturbance, increase in load demand or a change in system condition causes a progressive and uncontrollable drop in voltage [2]. Voltage instability is the cause of system collapse, in which the system voltage decays to a level from which it is unable to recover. Therefore, voltage stability analysis is important in order to identify the critical buses in a power system i.e., buses which are closed to their voltage stability limits and thus enable certain measures to be taken by the operators in order to avoid any incidence of voltage collapse [3], [4].

Over the last two decades the study of voltage instability problems has become an important and interesting area for

both researchers and utilities because of many incidents of system blackout caused by voltage collapse throughout the globe. Determination of the voltage stability limit of a complex power system is a difficult task and time consuming one. Fast computing techniques are needed to assess it to avoid the unwanted events of system operation. Several approaches have been reported in the open literature for predicting the voltage instability and collapse of the power system. Voltage stability being problem of power system under steady state operation, load flow study [5] has long been used to find voltage stability and security indicators. Continuation power flow technique [6] enables the researchers to identify critical point of voltage stability along with maximum system loadability. Load flow Jacobian, bifurcation analysis [7] has been proved to be the effective tools to identify voltage collapse point. Researchers also used the conventional P-V or Q-V curves [1] generated from the repetitive load flow solutions with successively increased load, for the assessment of voltage stability of the critical bus in a power system. A P-Q plane of stability is also used as a tool to assess the voltage stability limit of a power system [8].

Gradually the concept of deriving single line two-bus equivalent network [9]-[16] of any multi-bus power network has come up to get a quick overview on the system voltage stability in a global mode. Here, the actual system is reduced into an equivalent two-bus system and then the global voltage stability indices for indicating the state of the actual system are computed by using the parameters of the equivalent model. This concept is very attractive due to its simplicity and less computational effort and the occurrence of voltage collapse on the basis of the single line equivalent can be studied easily and it is not necessary to consider every line or bus of the system separately. Many researchers have developed the voltage stability indicators using the Thevenin's equivalent circuit [8], [10] to study the occurrence of voltage collapse of the actual system in global scenario. Some of the two-bus equivalent methodologies [11]-[16] developed are also capable to predict better scheme for strategic load shedding based on voltage stability criterion instead on the ground of simple voltage magnitude criterion.

In real time operation of power systems, the power control centers would have the information of the various system state measurements. Such information is similar to the result summary provided by the load flow or optimal power flow study. So the equivalent system can easily be evaluated and employed to assess the behavior of the system as a whole i.e.,

Dr. Nagendra Palukuru is with the Department of Technical Education (Govt. Polytechnic, Chandragiri), A.P., Hyderabad, India (e-mail: nagendra_ju@rediffmail.com).

Dr. Sunita Halder nee Dey, Dr. Subrata Paul, and Ms. T. Datta are with the Electrical Engineering Department, Jadavpur University, Kolkata-700032, West Bengal, India (e-mail: sunitaju@yahoo.com, speejupow@yahoo.co.in, tanayadatta21@yahoo.co.in).

in global mode without computation of Jacobian or Hessian matrix. Therefore, the representation of any multi-bus power system in an equivalent domain enables the fast assessment of voltage stability and so useful for the practical on-line monitoring of power systems.

Flexible AC transmission systems (FACTS), on the other hand, are being increasingly utilized to provide better voltage and power flow control in many utilities. They offer a versatile alternative to conventional methods with potential advantages of increased flexibility, lower operation and maintenance costs with less environmental impacts. Their application in improving the overall performance of the power system is discussed in [17], [18]. The most comprehensive controllers emanated from FACTS technology are static var compensator (SVC), static synchronous shunt compensator (STATCOM), thyristor controlled series compensator (TCSC) and static synchronous shunt compensator (SSSC) which provide an effective approach to improve the voltage stability and so the overall stability of the system. To analyze the effect of these controllers, steady state models have been developed over the decade. Load flow analysis using such models would provide data necessary to calculate the voltage stability indicators in order to evaluate the response of the system at any particular operating point.

With the concept of network equivalence available in literature, an attempt is made in this paper to describe the method of equivalencing a multi-bus power network to an equivalent two-bus system developed from the optimal power flow [19], [20] with integrated mathematical models of SVC and TCSC [16], [21], [22] and thereby voltage stable states of the entire system following the load changes in 'weak' load bus investigated for the typical power system network. Voltage stability margin enrichment with the application of SVC at the weakest bus and TCSC at critical line connected to the weakest bus is compared with the system having no compensation. Newton's method of optimal power flow has been utilized here to assess the voltage stability of the multi-bus power system considering economic criteria. The simulation also includes the detection of the weakest load bus [14], [23] and identification of the global voltage stable states of the system following the derived two-bus equivalent system. The proposed concept has been tested in a wide range of power networks of varying sizes. In this paper, a real life power system (Indian Eastern Grid WBSEB 203-bus) is used as the test system to illustrate the application of proposed method.

II. MODELING OF FACTS CONTROLLERS

With the advent of FACTS it has been possible for the power systems to operate with greater control of power, secure loading of transmission lines, prevention of cascading outages and damping of power system oscillations [17]. Among the important FACTS controllers, SVC and TCSC are most suitable for effective improvement of voltage stability. This paper presents the steady state models of SVC and TCSC controllers for OPF analysis, given in the following section.

A. Static var Compensator

Static var compensators have been extensively used in power system applications to provide the controlled reactive power and voltage stability improvement. The SVC firing angle model has been used here for optimal power flow analysis [21]. It is made up of the parallel combination of a thyristor controlled reactor (TCR) and a fixed capacitor. The SVC is connected to the transmission network via a step-down transformer as shown in Fig. 1.

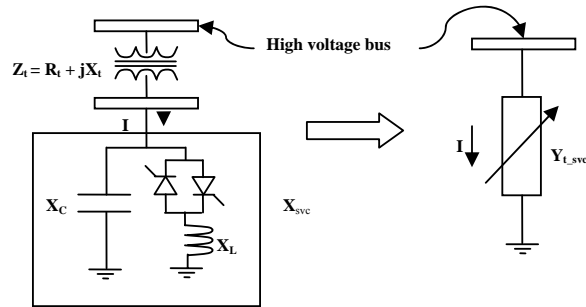


Fig. 1 SVC connected to the transmission network via a step-down transformer

The SVC is considered as a continuous, shunt variable susceptance, which is adjusted in order to achieve a specified voltage magnitude while satisfying constraint conditions. Suitable control of this equivalent reactance is brought about by varying the current through the TCR by controlling the gate firing instant of the thyristors and thus the equivalent susceptance B_{t_svc} is thus a function of the firing angle α . The SVC effective reactance X_{svc} is determined by the parallel combination of X_C and X_{tcr} and is given by

$$X_{svc} = \frac{X_C X_L}{\frac{X_C}{\pi} (2(\pi - \alpha) + \sin(2\alpha)) - X_L} \quad (1)$$

The partial derivatives required to calculate load flow Jacobian, with respect to the SVC (connected at m^{th} bus) firing angle α are,

$$\frac{\partial P_m}{\partial \alpha} = \frac{\partial P_{t_svc}}{\partial \alpha} = V_m^2 \frac{\partial G_{t_svc}}{\partial \alpha}$$

$$\frac{\partial Q_m}{\partial \alpha} = \frac{\partial Q_{t_svc}}{\partial \alpha} = -V_m^2 \frac{\partial B_{t_svc}}{\partial \alpha}$$

where net active power injected at node m is given by

$$P_m = \text{active power injected by lines connected to the node} + P_{t_svc}$$

and net reactive power injected at node m is given by

$$Q_m = \text{reactive power injected by lines connected to the node} + Q_{t_svc}$$

$$\text{Here, } G_{t_svc} + jB_{t_svc} = 1 / (R_t + j(X_t + X_{svc}))$$

The Lagrangian function including the α iteration model of SVC in OPF [20], [21] is given below where Q_m (SVC is connected to the m^{th} bus of the network) is a function of the thyristor firing angle α as well as bus voltage magnitudes $|V|$ and phase angles δ (transformer resistance R_t and hence G_{t_svc} is assumed to be negligible).

$$L(P_g, |V|, \delta) = \sum_{i=1}^{NG} F_c(P_{g_i}) + \sum_{i=1}^N \lambda_{p_i} [P_i(|V|, \delta) - P_{g_i} - P_{load_i}] + \sum_{i=NG+1}^N \lambda_{q_i} [Q_i(|V|, \delta) - Q_{g_i} - Q_{load_i}] + \lambda_{q_m} [Q_m(|V|, \delta, \alpha) - Q_{g_m} - Q_{load_m}] \quad (2)$$

If α is within limits ($90^\circ \leq \alpha \leq 180^\circ$), the specified voltage magnitude at the m^{th} bus is attained and it remains a PV bus-type. However, if α goes out of limits, it is fixed at the violated limit and the bus becomes a PQ type bus with fixed susceptance connected to it.

The Lagrangian function can be optimized using the following set of equations given in the matrix form:

$$\begin{bmatrix} \frac{\partial^2 L}{\partial P_g \partial P_g} & 0 & \frac{\partial^2 L}{\partial P_g \partial \lambda_{p_k}} & 0 & 0 & 0 \\ 0 & \frac{\partial^2 L}{\partial \alpha \partial \alpha} & \frac{\partial^2 L}{\partial \alpha \partial \lambda_{p_k}} & \frac{\partial^2 L}{\partial \alpha \partial \lambda_{q_k}} & \frac{\partial^2 L}{\partial \alpha \partial |V_k|} & 0 \\ \frac{\partial^2 L}{\partial \lambda_{p_i} \partial P_g} & \frac{\partial^2 L}{\partial \lambda_{p_i} \partial \alpha} & 0 & 0 & \frac{\partial^2 L}{\partial \lambda_{p_i} \partial |V_k|} & 0 \\ 0 & \frac{\partial^2 L}{\partial |V_i| \partial \alpha} & \frac{\partial^2 L}{\partial |V_i| \partial \lambda_{p_k}} & \frac{\partial^2 L}{\partial |V_i| \partial \lambda_{q_k}} & \frac{\partial^2 L}{\partial |V_i| \partial |V_k|} & 0 \\ 0 & \frac{\partial^2 L}{\partial \lambda_{q_i} \partial \alpha} & 0 & 0 & \frac{\partial^2 L}{\partial \lambda_{q_i} \partial |V_k|} & \frac{\partial^2 L}{\partial \lambda_{q_i} \partial \alpha} \\ 0 & 0 & 0 & \frac{\partial^2 L}{\partial \alpha \partial \lambda_{q_k}} & 0 & \frac{\partial^2 L}{\partial \alpha^2} \end{bmatrix} \begin{bmatrix} \Delta P_g \\ \Delta \alpha \\ \Delta \lambda_{p_i} \\ \Delta \lambda_{q_i} \\ \Delta |V_i| \\ \Delta \alpha \end{bmatrix} = \begin{bmatrix} \frac{\partial L}{\partial P_g} \\ \frac{\partial L}{\partial \alpha} \\ \frac{\partial L}{\partial \lambda_{p_i}} \\ \frac{\partial L}{\partial \lambda_{q_i}} \\ \frac{\partial L}{\partial |V_i|} \\ \frac{\partial L}{\partial \alpha} \end{bmatrix} \quad (3)$$

At the end of the i^{th} iteration, the variable firing angle α is updated like other state variables as, $\alpha^{i+1} = \alpha^i + \Delta \alpha^i$. G_{t_svc} and B_{t_svc} is calculated for the new value of firing angle α and hence the admittance matrix of the system is modified, incorporating the change in diagonal term Y_{mm} of the admittance matrix. However, if the new angle α violates any of the limits then it is fixed at the corresponding limit and α no longer serves as a state variable instead the voltage magnitude at bus m which was a specified variable now becomes a state variable.

B. Thyristor Controlled Series Compensator

TCSC is one of the most popular FACTS controllers, which allows rapid and continuous modulation of the transmission line impedance. Active power flows along compensated transmission line can be maintained at a specified value under a range of operating conditions [17]. Fig. 2 is a schematic

representation of TCSC which consists of a series capacitor in parallel with a thyristor controlled reactor (TCR). TCSC modifies the line reactance in order to control the power flow through the line.

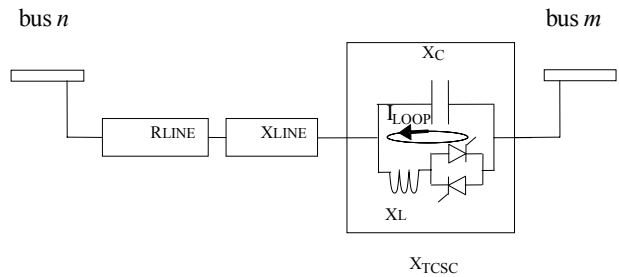


Fig. 2 TCSC connected between bus n and bus m

The equivalent reactance of the combination of fixed capacitor and thyristor controlled reactor is a function of the firing angle α of the TCR in TCSC and can be represented by the following equation [22],

$$X_{TCSC} = -X_C + C_1 \{2(\pi - \alpha) + \sin(2(\pi - \alpha))\} - C_2 \cos^2(\pi - \alpha) \{ \bar{\omega} \tan(\bar{\omega}(\pi - \alpha)) - \tan(\pi - \alpha) \} \quad (4)$$

where $C_1 = \frac{X_C + X_{LC}}{\pi}$; $C_2 = \frac{4X_{LC}^2}{X_L \pi}$; $\bar{\omega} = \frac{\omega_0}{\omega}$; $\omega_0 = \frac{1}{\sqrt{LC}}$;
 $X_{LC} = \frac{X_C X_L}{X_C - X_L}$; $\omega = 2\pi f$ and $90^\circ \leq \alpha \leq 180^\circ$

Thus for a line between any two buses n and m with TCSC in a system with N buses,

$$Z_{nm} = R_{LINE} + j(X_{LINE} + X_{TCSC})$$

So, Y_{nn} , Y_{nm} , Y_{mn} and Y_{mm} of the admittance matrix include $1/Z_{nm}$, of the line $n-m$. We can write,

$$\frac{1}{Z_{nm}} = \frac{1}{R_{LINE} + j(X_{LINE} + X_{TCSC})} = \frac{R_{LINE}}{DT} - j \frac{X_{eq}}{DT}$$

where $X_{eq} = (X_{LINE} + X_{TCSC})$ and $DT = (R_{LINE}^2 + X_{eq}^2)$

The inclusion of firing angle model of TCSC in optimal power flow formulation requires an additional constraint to maintain the power flow through the controlled line at the specified value. Active and reactive power injections at both the ends of the controlled line now becomes a function of thyristor firing angle α as well as bus voltage magnitudes $|V|$ and angles δ . So, the Lagrangian function can be modified as

$$L(P_g, |V|, \delta) = \sum_{i=1}^{NG} F_c(P_{gi}) + \sum_{i=1}^N \lambda_{pi} [P_i(|V|, \delta) - P_{gi} - P_{load_i}] + \sum_{i=NG+1}^N \lambda_{qi} [Q_i(|V|, \delta) - Q_{gi} - Q_{load_i}] + \mu [P_{nm}(|V|, \delta, \alpha) - P_{nm_{sp}}] \quad (5)$$

The equations necessary for solving optimal power flow including the TCSC at any particular line as per Newton's method can be written in matrix form as [19], [22]

$$\begin{bmatrix} \frac{\partial^2 L}{\partial P_{gi} \partial P_{gk}} & 0 & \frac{\partial^2 L}{\partial P_{gi} \partial \lambda_{pk}} & 0 & 0 & 0 & 0 \\ 0 & \frac{\partial^2 L}{\partial \delta_i \partial \delta_k} & \frac{\partial^2 L}{\partial \delta_i \partial \lambda_{pk}} & \frac{\partial^2 L}{\partial \delta_i \partial \lambda_{qk}} & \frac{\partial^2 L}{\partial \delta_i \partial |V_k|} & \frac{\partial^2 L}{\partial \delta_i \partial \mu} & \frac{\partial^2 L}{\partial \delta_i \partial \alpha} \\ \frac{\partial^2 L}{\partial \lambda_{pi} \partial P_{gk}} & \frac{\partial^2 L}{\partial \lambda_{pi} \partial \delta_k} & 0 & 0 & \frac{\partial^2 L}{\partial \lambda_{pi} \partial |V_k|} & 0 & \frac{\partial^2 L}{\partial \lambda_{pi} \partial \alpha} \\ 0 & \frac{\partial^2 L}{\partial |V_i| \partial \delta_k} & \frac{\partial^2 L}{\partial |V_i| \partial \lambda_{pk}} & \frac{\partial^2 L}{\partial |V_i| \partial \lambda_{qk}} & \frac{\partial^2 L}{\partial |V_i| \partial |V_k|} & \frac{\partial^2 L}{\partial |V_i| \partial \mu} & \frac{\partial^2 L}{\partial |V_i| \partial \alpha} \\ 0 & \frac{\partial^2 L}{\partial \alpha_i \partial \delta_k} & 0 & 0 & \frac{\partial^2 L}{\partial \alpha_i \partial |V_k|} & 0 & \frac{\partial^2 L}{\partial \alpha_i \partial \alpha} \\ 0 & \frac{\partial^2 L}{\partial \mu \partial \delta_k} & 0 & 0 & \frac{\partial^2 L}{\partial \mu \partial |V_k|} & 0 & \frac{\partial^2 L}{\partial \mu \partial \alpha} \\ 0 & \frac{\partial^2 L}{\partial \alpha \partial \delta_k} & \frac{\partial^2 L}{\partial \alpha \partial \lambda_{pk}} & \frac{\partial^2 L}{\partial \alpha \partial \lambda_{qk}} & \frac{\partial^2 L}{\partial \alpha \partial |V_k|} & \frac{\partial^2 L}{\partial \alpha \partial \mu} & \frac{\partial^2 L}{\partial \alpha \partial \alpha} \end{bmatrix} \begin{bmatrix} \Delta P_{gi} \\ \Delta \delta_i \\ \Delta \lambda_{pi} \\ \Delta \lambda_{qi} \\ \Delta |V_i| \\ \Delta \mu \\ \Delta \alpha \end{bmatrix} = \begin{bmatrix} \frac{\partial L}{\partial P_{gi}} \\ \frac{\partial L}{\partial \delta_i} \\ \frac{\partial L}{\partial \lambda_{pi}} \\ \frac{\partial L}{\partial \lambda_{qi}} \\ \frac{\partial L}{\partial |V_i|} \\ \frac{\partial L}{\partial \mu} \\ \frac{\partial L}{\partial \alpha} \end{bmatrix} \quad (6)$$

At the end of the i^{th} iteration, the variable firing angle α and Lagrangian multiplier μ is updated like other state variables as, $\alpha^{i+1} = \alpha^i + \Delta \alpha^i$ and $\mu^{i+1} = \mu^i + \Delta \mu^i$. X_{TCSC} is calculated for the new value of firing angle α and hence the admittance matrix of the system is modified, incorporating the change in diagonal term Y_{mm} , Y_{nn} and off-diagonal term Y_{nm} and Y_{mn} of the admittance matrix. If α is within limits ($90^\circ \leq \alpha \leq 180^\circ$), the specified active power flow is attained. However, if α goes out of limits, it is fixed at violated limit and active power flow through the line is uncontrolled determined by fixed reactance of the TCSC.

The total power loss of the entire multi-bus power network being the algebraic sum of all line flows in the system, the power balance equation for multi-bus power system is given by

$$S_g = S_{load} + S_l \quad \text{also,} \quad S_l = S_{se} + S_{sh}$$

where S_l is total complex power loss; S_{se} , S_{sh} are total complex series and shunt losses; S_g , S_{load} are total complex source and load powers respectively.

III. EQUIVALENT TWO-BUS SYSTEM AND FORMULATION OF GLOBAL VOLTAGE STABILITY INDICATOR

Two-bus equivalent model for any multi-bus power system is obtained using the total generation, load and loss available from optimal power flow analysis for a particular operating

condition where none of the two buses are actually present in the system as in [11], [12] as shown in Fig. 3.

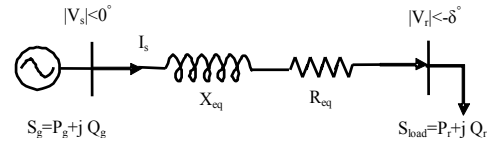


Fig. 3 Equivalent two-bus power network

The behavior of equivalent system is the same as that of multi-bus power network and reflects the common properties of actual system and makes possible the evaluation of voltage stability. Therefore, the power balance equation for the two bus equivalent network can be written as

$$S_g = S_{load} + S_{loss} \\ \text{i.e.,} \quad P_g + jQ_g = \overline{V}_s \overline{I}_s^* = (P_{loss} + jQ_{loss}) + (P_r + jQ_r) \\ \therefore |\overline{I}_s|^2 = \frac{(P_g^2 + Q_g^2)}{|\overline{V}_s|^2} \\ R_{eq} = \frac{P_{loss}}{|\overline{I}_s|^2} = \frac{P_{loss}}{(P_g^2 + Q_g^2)} |\overline{V}_s|^2 \\ \text{and} \quad X_{eq} = \frac{Q_{loss}}{|\overline{I}_s|^2} = \frac{Q_{loss}}{(P_g^2 + Q_g^2)} |\overline{V}_s|^2 \quad (7)$$

So,

Then, the receiving end voltage V_r can easily be calculated as follows:

$$|\overline{V}_r| = |\overline{V}_s| - (R_{eq} + jX_{eq}) \left(\frac{P_g - jQ_g}{|\overline{V}_s|^*} \right) \quad (8)$$

where V_s and I_s are the sending end voltage and current; S_g , S_{load} are the total complex source and load powers respectively; S_{loss} is the total complex loss in the power system.

All the parameters of the equivalent two-bus network can be obtained by assuming $\overline{V}_s = 1 \angle 0^\circ$ p.u. and thus the equivalent model of multi-bus power system is developed at any particular network and load configuration where the total interconnected system has been replaced by a single line two bus system with same generation, load and loss.

Once the global two-bus power network equivalent to multi-bus power system is obtained, and then the global voltage stability margin (GVSM) could be formulated in a straight forward manner from parameters of the global network as described below:

The $ABCD$ parameters for the two-bus series equivalent system is given by

$$\begin{bmatrix} A & B \\ C & D \end{bmatrix} = \begin{bmatrix} 1 & Z_{eq} \\ 0 & 1 \end{bmatrix}$$

Assuming $B = |B| \angle \beta$; $V_r = |V_r| \angle -\delta$ and the sending end voltage, V_s being constant ($1 \angle 0^\circ$ p.u.), the active and reactive power at the receiving end are given by

$$P_r = \frac{|V_r|}{|B|} \cos(\beta + \delta) - \frac{|V_r|^2}{|B|} \cos \beta \quad (9)$$

$$Q_r = \frac{|V_r|}{|B|} \sin(\beta + \delta) - \frac{|V_r|^2}{|B|} \sin \beta \quad (10)$$

The jacobian matrix [20] of above power flow equation is given by

$$J = \begin{bmatrix} \frac{\partial P_r}{\partial \delta} & \frac{\partial P_r}{\partial V_r} \\ \frac{\partial Q_r}{\partial \delta} & \frac{\partial Q_r}{\partial V_r} \end{bmatrix}$$

Then, the determinant of jacobian matrix,

$$\Delta[J] = \frac{1}{B} [2AV_r^2 \cos \delta - V_r] \quad (11)$$

At the critical point of voltage stability, $\Delta[J] = 0$

$$\therefore V_r = V_{cr} = \frac{1}{2 \cos \delta_{cr}} \quad (12)$$

where V_{cr} is the critical value of receiving end voltage at voltage stability limit. Lower value of V_{cr} indicates the system will have better voltage profile along with higher load catering capability and therefore better voltage stability.

At the critical point of voltage stability, $\Delta[J] = 0$; and so to maintain the global voltage stability, $\Delta[J] > 0$; Therefore to secure global voltage stability, global voltage stability margin can be defined as $GVSM = \Delta[J]$. It indicates how far the present operating condition is from global system voltage collapse i.e., GVSM points on the global voltage security status of the present operating condition.

IV. COMPUTATIONAL ALGORITHM

The proposed algorithm for the system simulation is given below:

- Step 1. Run the base case OPF and determine the weakest bus of the given multi-bus system.
- Step 2. Make necessary modifications in the bus admittance matrix and Hessian matrix for incorporating SVC or TCSC.
- Step 3. Solve optimal power flow problem to obtain the system states. Go to step 6 if OPF iterative process does not converge.
- Step 4. Calculate the total generation, load and transmission line loss of the system. Calculate equivalent resistance (R_{eq}) and equivalent reactance (X_{eq}) and other

parameters for the two-bus equivalent model and hence the global voltage stability margin (GVSM).

Step 5. Increase the load of weakest bus by small steps at a constant power factor and go to step-3.

Step 6. Stop.

V. SIMULATION RESULTS

The proposed algorithm has been presented here using the West Bengal State Electricity Board (WBSEB) 203-bus Indian Eastern Grid system, which has a base load of 8887.48 MVA with 24 generators, 35 three-winding transformers, 37 two-winding transformers and 108 load buses which are interconnected by 267 transmission lines. The single line diagram of the test system is given in Appendix A. A computer software program has been developed in the MATLAB environment to perform the optimal power flow analysis including the above discussed models of SVC and TCSC. The reactive power sensitivity analysis (dQ/dV criterion) [14], [23] is used here to diagnose the weakest bus of the system and the load bus having minimum reactive power sensitivity is assumed to be the weakest bus. This analysis reveals that bus number 172 as the weakest bus of the system. Proposed methodology is applicable to any load bus of the test system; the weakest bus is chosen here to present the simulation as it has highest sensitivity towards voltage stability.

First, the optimal power flow is successively solved for uniformly increasing load conditions (at an increment of 20% of base value keeping the load power factor constant) at the weakest bus until the OPF algorithm fails to converge. The OPF problem is then similarly solved for the application of SVC at the weakest bus or TCSC at critical line connected to the weakest bus. It should be noted that only one FACTS controller at a time has been considered here for the simulation purpose. For each case and each load set, the parameters of two-bus equivalent model have been calculated and have been used to assess the voltage stability of the actual system in global scenario by calculating the global voltage stability margin and global receiving end voltage. The data used for SVC and TCSC controllers is given in appendix B. The results are quite encouraging and promising to assess the voltage stability of any power system at any operating point in global mode, which are enlighten by the profiles shown below.

Fig. 4 exhibits the profile of global voltage stability margin (GVSM) for WBSEB grid system indicating that the system gradually moves towards voltage instability with increase in load. Improved profiles have been obtained with the application of FACTS devices. It is clear from figure that with the incorporation of SVC at weakest bus (no. 172) of the system, the GVSM has been improved with better loading catering capability. It is also observed here that with the application of TCSC in a critical line (line no. 21 which is connected between buses 156 and 152), more power flow than original is possible at each load set. TCSC enables the system to transmit more power maintaining global voltage stability.

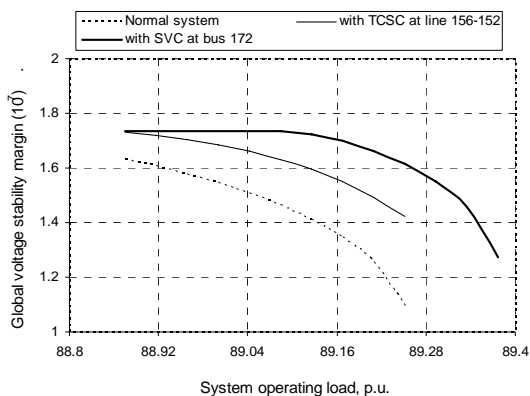


Fig. 4 Profile of global voltage stability margin with the variation of system operating load

This is clear that the value of GVSM is very high at the maximum loading point as it has been calculated from the equivalent two-bus model of the actual system for which the parameters of the equivalent system vary with variation of system operating condition. And, beyond the maximum loading point the value of GVSM becomes zero indicating that the system moving towards voltage instability. Still a set of pre-calculated values of the GVSM corresponds to the collapse points for different operating condition may be useful for the real time operation where only the total line loss, total generation and total load of entire system will be sufficient for calculating the present indicator value from the measured system data which on comparison with the already pre-calculated GVSM data may reveal whether system is at the verge of voltage collapse or not, almost instantly. Thus this approach may be beneficial due to its simplicity associated with high speed of decision making.

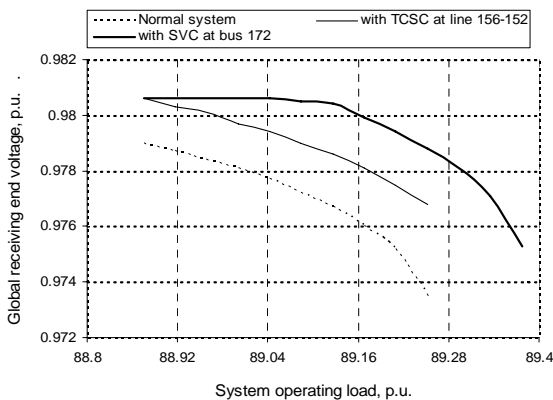


Fig. 5 Profile of global receiving end voltage with the variation of system operating load

The profile in Fig. 5 reveals that global receiving end voltage (V_g) for the equivalent two-bus system is gradually decreasing with enhancement of load indicating the system is approaching towards local voltage collapse at equivalent receiving end. It is clear from figure that with the inclusion of SVC, there is sharp improvement in voltage stability along

with higher loading capability. Also, the application of TCSC indicates improved voltage profile though its actual significance lies in its capability of handling increased power flow and hence increased stability even under stressed condition.

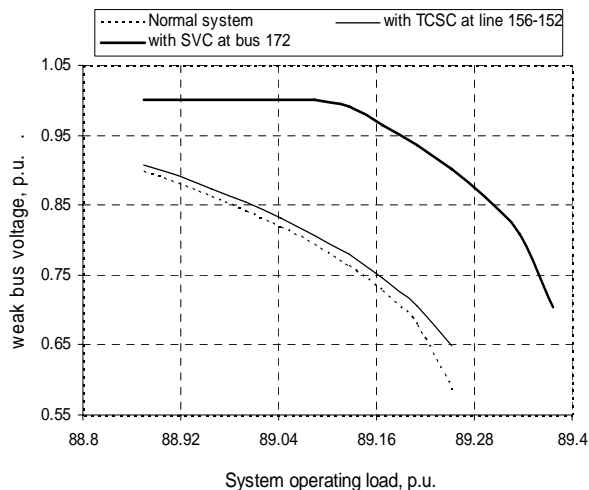


Fig. 6 Profile of weak bus voltage with the variation of system operating load

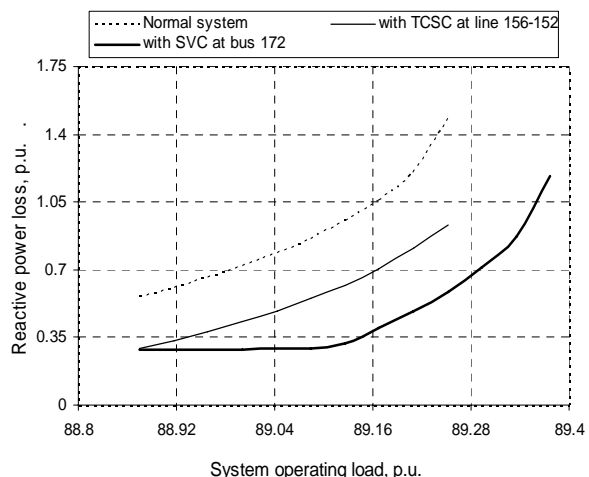


Fig. 7 Variation of reactive power loss with the variation of system operating load

The bus voltage magnitude in Fig. 6 reveals that the voltage corresponding to the weakest bus gradually decreasing and thereby it approaches voltage instability for increase in system loading. A flatter voltage profile is possible where SVC is connected at the weakest bus of the system with better load handling capacity. The bus voltage starts drooping when SVC reaches its firing angle limit. Fig. 6 also suggests that an improvement in voltage profile is possible at all operating conditions with the incorporation of TCSC. It is observed here that the voltage profile is significantly improved with the insertion of SVC compared to TCSC.

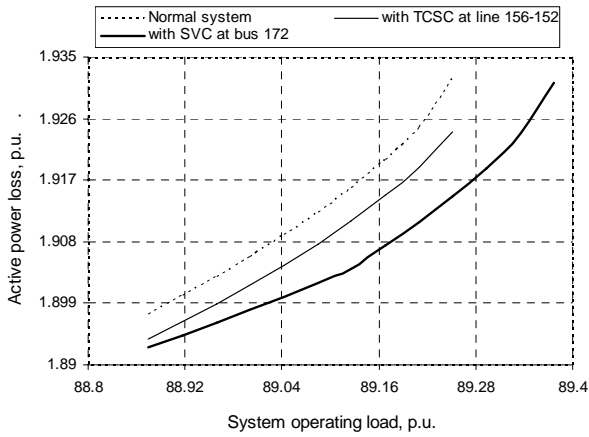


Fig. 8 Variation of active power loss with the variation of system operating load

Figs. 7 and 8 exhibit the profiles of reactive power loss and active power loss respectively, for variation of the system operating load indicating that the losses are reduced with the application of FACTS devices. Moreover, it is observed from

figures that with the application of SVC the losses are reduced in a better way compared to TCSC under every operating condition.

VI. CONCLUSION

A global two-bus network equivalent to assess the voltage stability of a multi-bus power system based on the optimal power flow has been developed. The operating variables of the developed two-bus equivalent network are employed to assess the voltage stability of the actual system in global scenario. Also, detailed steady state models of SVC and TCSC have been developed and integrated into OPF program to investigate their impact on voltage stability and security of any multi-bus power system. The simulation results clearly demonstrate that representation of any multi-bus power network in an equivalent domain is very useful to assess the overall voltage stability status of the system. Incorporation of SVC and TCSC controllers in OPF analysis helps to examine their influence in equivalent domain and therefore in global voltage stability which in due course helps the system operator to take quick action for particular voltage stability related problem.

APPENDIX A

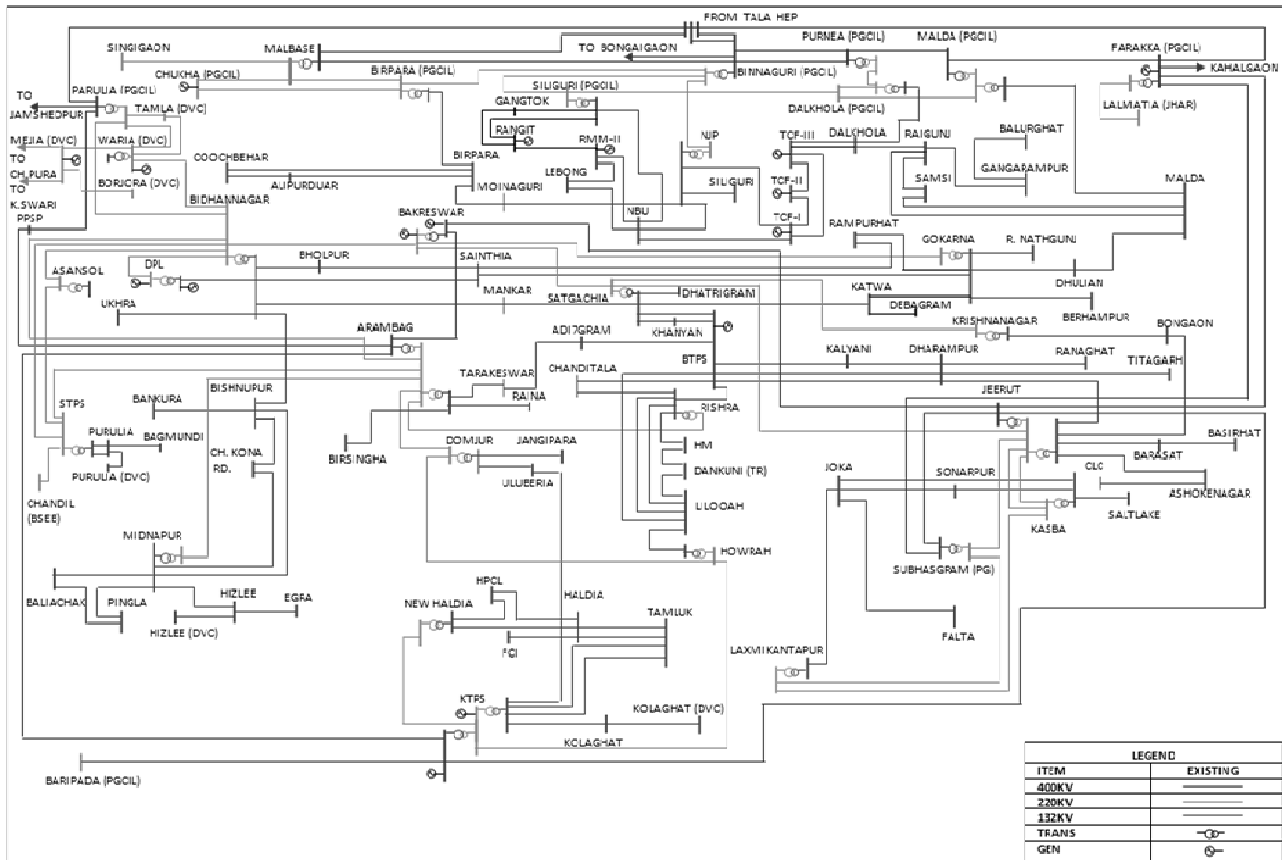


Fig. 9 Typical Indian Eastern Grid (WBSEB 203-bus) system

APPENDIX B

The SVC parameters adopted are:

- 1) Transformer reactance $X_T=0.334$ p.u.
- 2) Transformer resistance $R_T=0$ p.u.
- 3) Inductor reactance for the TCR, $X_L=0.8741$ p.u. and
- 4) Capacitive reactance, $X_C=3.2484$ p.u.

The maximum capacitive susceptance obtained is $B_{SVC\ max} = 0.3431$ p.u. i.e. 34.31 MVar is the maximum reactive power that the SVC can inject at 1.00 p.u. terminal voltage. Resonance for the values adopted for the SVC model occurs at about 128° . Thus an initial value of 140° has been adopted for the firing angle α .

The TCSC parameters adopted for line number 21, connected between buses 156-152 of WBSEB system with line resistance 0.0034 p.u. and line reactance 0.0128 p.u. are:

- 1) Capacitive reactance, $X_C=0.005$ p.u. and
- 2) Inductive reactance $X_L=0.00135$ p.u. for which resonance occurs at 133.2346° .

REFERENCES

- [1] T. Van Cutsem, and C. Vournas, *Voltage stability of electric power systems*. Bostan, Kluwer Academic Publishers, 1998.
- [2] T. Van Cutsem, "A method to compute reactive power margins with respect to voltage collapse," *IEEE Trans. Power System*, vol. 6, no. 1, pp. 145-156, Feb. 1991.
- [3] Q. Wang, and V. Ajjarapu, "A critical review on preventive and corrective control against voltage collapse," *Electric Power Components and Systems*, vol. 29, no. 12, pp. 1133-1144, Dec. 2001.
- [4] M. Z. El-Sadek, M. S. Abdel-Salam, A. A. Ibraheem, and A. A. Hussein, "Criteria for determination of steady state voltage stability of power systems," *Electric Power Components and Systems*, vol. 25, pp. 851-864, 1997.
- [5] P. W. sauer, and M. A. Pai, "Power system steady state stability and the load flow Jacobian," *IEEE Trans. Power systems*, vol. 5, no. 4, pp. 1374-1383, Nov. 1990.
- [6] V. Ajjarapu, and C. Christy, "The continuation power flow: a tool for steady state voltage stability assessment", *IEEE Trans. Power systems*, vol. 7, no.1, pp. 416-423, Feb. 1992.
- [7] C. A. Canizares, "On bifurcations, voltage collapse and load modeling," *IEEE Trans. Power systems*, vol. 10, no.1, pp. 512-522, Feb. 1995.
- [8] M. H. Haque, "Novel method of assessing voltage stability of a power system using stability boundary in a P-Q plane," *Electric Power Systems Research*, vol. 64, no. 1, pp. 35-40, Jan. 2003.
- [9] P. Nagendra, T. Datta, S. Halder, and S. Paul, "Power system voltage stability assessment using network equivalents-A review," *Journal of Applied Sciences*, vol. 10, no. 18, pp. 2147-2153, 2010.
- [10] A. M. Chebbo, M. R. Irving, and M. J. H. Sterling, "Voltage collapse proximity indicator: Behavior and implications," *IEE Proc. C Gen. Trans. Distr.*, vol. 139, no. 3, pp. 241-252, May 1992.
- [11] B. Jasmon, and L. H. C. C. Lee, "Distribution network reduction for voltage stability analysis and load flow calculation," *Int. J. Elec. Power and Energy Syst.*, vol. 13, no. 1, pp. 9-13, Feb. 1991.
- [12] M. Moghavvemi, and M. O. Faruque, "Power system security and voltage collapse: a line outage based indicator for prediction," *Int. J. Elec. Power and Energy Syst.*, vol. 21, no. 6, pp. 455-461, Aug. 1999.
- [13] F.Gubina, and B. Strmcnik, "A simple approach to voltage stability assessment in radial networks," *IEEE Trans. Power systems*, vol. 12, no. 3, pp. 1121-1128, Aug. 1997.
- [14] S. Dey, C. K. Chanda, and A. Chakrabarti, "Development of a concept of global voltage security indicator (VSI) and role of SVC on it in longitudinal power supply (LPS)," *Electric Power System Research*, vol. 68, no.1, pp. 1-9, Jan. 2004.
- [15] P. Nagendra, S. Halder nee Dey, and S. Paul, "OPF based voltage stability assessment of a power system using network equivalencing technique," in *Proc. 3rd Int Conf on Power Systems*, IIT Kharagpur, India, 2009.
- [16] P. Nagendra, S. Halder nee Dey, T. Datta and S. Paul, "On-line voltage stability assessment in the presence of TCSC with economic consideration," in *Proc. 2010 Annual IEEE India Conference (INDICON)*, Jadavpur University, Kolkata, India, 2010.
- [17] N. G. Hingorani, and L. Gyugyi, *Understanding FACTS: Concepts and Technology of Flexible AC Transmission System*, Wiley-IEEE Press, 1999.
- [18] M. A. Abido, "Power system stability enhancement using FACTS controllers: A review," *The Arabian Journal for Science and Engineering*, vol. 34, no. 1B, pp.153-172, Apr. 2009.
- [19] David I. Sun, B. Ashley, B. Brewer, A. Hughes, and W. F. Tinney, "Optimal power flow by Newton approach," *IEEE Trans. Power App. system*, PAS-103, no. 10, pp. 2864-2880, Oct. 1984.
- [20] A. Chakrabarti, and Sunita Halder, *Power System Analysis: Operation and Control*, 2nd ed., PHI Ltd., India, 2008.
- [21] H. Ambriz-Perez, E. Acha, and C. R. Fuerte-Esquivel, "Advanced SVC models for Newton-Raphson load flow and Newton optimal power flow studies," *IEEE Trans. Power system.*, vol.15, pp. 129-136, 2000.
- [22] H. Ambriz-Perez, E. Acha, and C. R. Fuerte-Esquivel, "TCSC-firing angle model for optimal power flow solutions using Newton's method," *Int. J. Electric Power and Energy System*, vol. 28, pp. 77-85, 2006.
- [23] A. Chakrabarti, D. P. Kothari, A. K. Mukhopadhyay, and A. De, "An Introduction to Reactive Power Control and Voltage Stability in Power Transmission Systems," PHI Ltd., India, 2010.